# Anticrossing and coupling of light-hole and heavy-hole states in (001) GaAs/Al$_x$Ga$_{1-x}$As heterostructures

Rita Magri

*Istituto Nazionale per la Fisica della Materia e Dipartimento di Fisica, Università di Modena e Reggio Emilia, Modena, Italy*

Alex Zunger

*National Renewable Energy Laboratory, Golden, Colorado 80401l*

Heterostructures sharing a common atom such as AlAs/GaAs/AlAs have a $D_{2d}$ point-group symmetry which allows the bulk-forbidden coupling between odd-parity light-hole states e.g., lh1) and even-parity heavy-hole states e.g., hh2). Continuum models, such as the commonly implemented ''standard model'') $\mathbf{k} \cdot \mathbf{p}$ theory miss the correct $D_{2d}$ symmetry and thus produce zero coupling at the zone center. We have used the atomistic empirical pseudopotential theory to study the lh1-hh2 coupling in 001) superlattices and quantum wells of GaAs/Al$_x$Ga$_{1-x}$As. By varying the Al concentration $x$ of the barrier we scan a range of valence-band barrier heights $E_v(x)$. We find the following: i) The lh1 and hh2 states anticross at rather large quantum wells width or superlattice periods $60 < n_c < 70$ monolayers. ii) The coupling matrix elements $V_{lh1,hh2}^{\mathbf{k}_\parallel=0}$ are small 0.02–0.07 meV) and reach a maximum value at a valence-band barrier height $E_v \approx 100$ meV, which corresponds to an Al composition $x_{Al} = 0.2$ in the barrier. iii) The coupling matrix elements obtained from our atomistic theory are at least an order of magnitude smaller than those calculated by the phenomenological model of Ivchenko *et al.* Phys. Rev. B **54**, 5852 1996)]. iv) The dependence of $V_{lh1,hh2}$ on the barrier height $E_v(x)$ is more complicated than that suggested by the recent model of Cortez *et al.*, J. Vac. Sci. Technol. B **18**, 2232 2000)], in which $V_{lh1,hh2}$ is proportional to the product of $E_v(x)$ times the amplitudes of the lh1 and hh2 envelopes at the interfaces. Thus, atomistic information is needed to establish the actual scaling.

## I. INTRODUCTION

### A. The three classes of light-hole−heavy-hole coupling in semiconductor heterostructures

Quantum states that belong to the same symmetry representation mix and anticross in the presence of a perturbation. The anticrossing effect on electronic energy levels of solids is often very significant, and includes the occurrence of ''band-gap bowing'' in random alloys,[1] band-gap narrowing in ordered vs random alloys,[2] saturation of impurity levels with pressure,[3] and ''$p$-$d$ repulsion'' in II-VI Ref. 4) or I-III-VI$_2$ Ref. 5) compounds affecting band offsets and spin-orbit splitting. Here we focus on the consequences of level anticrossing in 001) semiconductor superlattices and quantum wells made of zinc-blende constituents. In the zinc-blende structure the valence-band maximum VBM) is a four-degenerate $\Gamma_{8v}$ state including~hh!components. The optical transitions lh to the first electron level $e$ are allowed in the bulk and have isotropic polarization. When one forms a 001)-oriented quantum well from zinc-blende components, there are three different effects on the electronic states: i) The zinc-blende bands between $\Gamma$(000) and $X$(001) fold into $\mathbf{k}_\parallel = 0$ of the quantum well thus adding new states, ii) the reduced superlattice symmetry from $T_d$ can split $\Gamma_{8v}$, and iii) the strain arising from size mismatch can also split $\Gamma_{8v}$. This last effect is absent in lattice-matched components such as GaAs and AlAs. In GaAs/AlAs heterostructures effects i) and ii)

give rise to a series of hole levels hh1 < lh1 < hh2 . . . and electron states $e1 < e2 < . . .$ at $\mathbf{k}_\parallel = 0$.

Coupling exists between states of the same symmetry. This is decided as follows. A *single* zinc-blende 001) interface has $C_{2v}$ symmetry.[6] If one forms a structurally perfect

TABLE I. Light-hole and heavy-hole couplings at $k_\parallel=0$ for the first three subbands in common and no-common atom zinc-blende heterostructures grown along the [001] axis. $V_{lh1,hh1}$ is responsible for the in-plane polarization anisotropy [PA] [Eq. (1)] of the interband transitions to electron states, while the $V_{lh1,hh2}$ coupling is responsible for the appearance of $lh1$-$e2$ and $hh2$-$e1$ forbidden transitions. Standard $\mathbf{k}\cdot\mathbf{p}$ implementations produce $V_{lh,hh}=0$ at $k_\parallel=0$ in all of the cases below.

| System | $V_{lh1,hh1}$ | $V_{lh1,hh2}$ | PA |
|---|---|---|---|
| A single [001] interface, e.g., [AlAs/GaAs]: $C_{2v}$ | nonzero | nonzero | 0 |

ropy $\neq 0$. The nature of the level mixing depends on symmetry. There are three cases: i) A single zinc-blende interface; the symmetry is $C_{2v}$. ii) Two different interfaces in systems that do not share a common atom; the symmetry is $C_{2v}$. iii) Two interfaces in systems that share a common atom; the symmetry is $D_{2d}$. Two equal interfaces in no-common atom systems in [001] superlattices with a noninteger period also have $D_{2d}$ symmetry. We next describe briefly these cases summarized in Table I. In this paper we concentrate mainly on case [iii)].

i) *A single zinc-blende interface: $C_{2v}$*. A single interface can be grown intentionally. Alternatively, if two interfaces of a quantum well made of common-atom pair have some growth defect [e.g., due to segregation], then the combined $C_{2v}$ symmetries of the individual interfaces do not add up to a $D_{2d}$ symmetry, but instead the $C_{2v}$ symmetry of a single interface survives. Even if the two interfaces are defect-free, one can break the symmetry relation of the two interfaces in a quantum well by applying an electric field in the growth direction. In all of these cases the lower $C_{2v}$ symmetry breaks the degeneracy at the VBM and leads to a coupling between the components of $\Gamma_{8v}$ at $k_\parallel=0$. In a quantum well or superlattice where the states are described as the product of a Bloch state of the zinc-blende parent compound at $k_\parallel=0$ times an envelope function, this mixing is translated into the coupling of the states which have the same symmetry representation under $C_{2v}$ [and thus can mix and anticross]. These are $lhn$ and $hhm$ for *any* quantum index $n$ and $m$. Thus, $lh1$ can mix with $hh1$ in $C_{2v}$. As a consequence of these mixings, parity-forbidden transitions and an in-plane polarization anisotropy of the optical properties can be observed. This was seen in photoluminescence and reflectance difference spectroscopy experiments on GaAs/AlAs after the application of an electric field along the growth direction [the quantum confined Pockels effect[8,9]] or in the case of AlAs/GaAs/Al$_x$Ga$_{1-x}$As asymmetric quantum wells.[10] The effect of the electric field on common atom GaAs/AlAs quantum wells is twofold: a) by lowering the symmetry to $C_{2v}$ it allows the mixing of $lh$ and $hh$ states with the same parity [i.e., $lh1$ and $hh1$], b) the field breaks the parity symmetry of all the hole and electron states and allows the $lh1$ and $hh2$ coupling to be observed experimentally through a strong polarization anisotropy of the emission of the nominally forbidden excitons [i.e., $hh2$-$e1$ and $hh1$-$e2$].[8]

Among the experimental studies addressing the symmetry properties of the single [001] interface is the work of Gour-don and Lavallard[11] who studied the features of a previously reported small splitting [a few $\mu$eV] of heavy excitons in type-II GaAs/AlAs superlattices. The authors could account for the observed splitting by assuming that the superlattice had a $C_{2v}$ symmetry, not the nominal $D_{2d}$ symmetry. The physical origin of the $C_{2v}$ symmetry was attributed to different degrees of interfacial roughness which causes an asymmetry between the [110] and [$-110$] directions at the [001] interfaces, together with the biaxial compression of the AlAs layers. Another paper addressing the additional exchange splitting in type-II GaAs/AlAs superlattices is the theoretical work of Pikus and Pikus,[12] who have proposed two models to explain the origin of the symmetry reduction to $C_{2v}$ and hole mixing: a local deformation in the GaAs well, or the fact that localized exciton in type-II short-period structures sees only one interface. Edwards and Inkson,[13] using an empirical pseudopotential formalism, studied the hole scattering at a [001] GaAs/AlAs single interface ($C_{2v}$), and found a strong bulk light-hole–heavy-hole mixing at $k_\parallel=0$.

ii) *Two interfaces that do not share a common atom: $C_{2v}$* This case corresponds to no-common atom InAs/GaSb or [GaIn]As/InP systems with two different interfaces discussed in Refs. 7,14–16. In this case a giant in-plane optical anisotropy has been found in absorption measurements[7] even *without* application of electric fields. The asymmetric potential along the growth direction is supplied by the inequivalence of the [001] interfaces which lowers the overall symmetry from $D_{2d}$ to the $C_{2v}$ point group. The anisotropy is largest at the onset of absorption in type-I superlattices [GaIn]As/InP implying[7] a strong coupling between $hh1$ and $lh1$ at the top of the valence band at $k_\parallel=0$. Recently the polarization anisotropy in no-common atom systems has been investigated by atomistic *ab initio*[14] and semiempirical[15,16] pseudopotential methods. An atomistic semiempirical pseudopotential scheme[15] has indeed found a polarization anisotropy of the $h1$-$e1$ transition at $k_\parallel=0$ in type-II semiconducting InAs/GaSb superlattices. Note that this anisotropy cannot be predicted by "standard" $\mathbf{k}\cdot\mathbf{p}$ theories which produce zero heavy and light hole coupling, $V_{lh,hh}=0$, at $k_\parallel=0$. A consequence of $hh1$ and $lh1$ coupling in the real InAs/GaSb systems is the occurrence of nonzero coupling $V_{e1,hh1}\neq 0$ between the electron state $e1$ and the heavy-hole state $hh1$ at $k_\parallel=0$ found for superlattices $(InAs)_n/(GaSb)_n$ with $n \approx 28$.[15] The eight band $\mathbf{k}\cdot\mathbf{p}$ theory, which yields $V_{e1,hh1}^{k_\parallel=0}=0$, has predicted instead a simple crossing. On the other

hand, the $\mathbf{k} \cdot \mathbf{p}$ theory is capable of describing couplings at $\mathbf{k}_\parallel$ 0 and thus has produced results similar to those of atomistic theories for the hibridization gaps at $\mathbf{k}_\parallel$ 0 in nominally semimetallic $(\text{InAs})_n /(\text{GaSb})_n$ superlattices with $n > 28$.[16]

iii) *Two interfaces of a common-atom heterostructure:* $D_{2d}$. The states that have the same symmetry representation and hence can mix and anticross) under $D_{2d}$ are hh even with lh odd such as hh2 and lh1) or hh odd with lh even such as hh1-lh2). The lh1-hh1 coupling is forbidden. In the $D_{2d}$

priate $C_{2v}$ symmetry of the single 001) interface. This approach is substantially similar to Ivchenko's. The only difference is that the lh-hh coupling parameter is expressed in terms of the valence-band offset.[27]

## C. The purpose of the present paper and its main results

The purpose of this paper is to provide a microscopic atomistic theory for lh1-hh2 coupling in $D_{2d}$-type GaAs/ AlGa)As heterostructures. Using the empirical pseudopotential method we determine the period $n_c$ where the $(GaAs)_n/(AlAs)_n$ superlattices and the $(GaAs)_n/(Al_{1-x}Ga_xAs)$ quantum wells exhibit lh1-hh2 anticrossing at different values $x$ of the barrier. By varying the composition of the barrier material we alter the magnitude of the well-to-barrier valence-band offset $E_v(x)$. Calculation of the coupling matrix element vs barrier composition then establishes $V_{lh1,hh2}^{\mathbf{k}_\parallel=0}$ for different barrier heights $E_v(x)$. We find that: i) the lh1 and hh2 states anticross at rather large quantum well widths or superlattice periods $60 < n_c < 70$ monolayers. ii) The coupling matrix element $V_{lh1,hh2}^{\mathbf{k}_\parallel=0}$ is small, being between 0.02 meV and 0.07 meV. iii) The coupling matrix element obtained from our atomistic theory is at least an order of magnitude smaller than that inferred from the phenomenological model Hamiltonian approach of Ivchenko using a coupling parameter $t_{lh}=0.5$).[6] iv) The coupling matrix element is small at low Al composition shallow barrier)

tonian; d) one needs to fit only the bulk band structure without additional e.g., interfacial) parameters[6].

Finally, using the eigenstates obtained solving Eq. 2) we have calculated the interband dipole transitions-matrix elements squared $I_{i,j}(\hat{}) = |\langle_i|\hat{}\cdot\hat{p}|_j\rangle|^2$, where $\hat{}$ is the photon polarization vector, $_i$ are the hh1, lh1, and hh2 hole states, while $_j$ are the $e1$ and $e2$ electron states at $\mathbf{k}_\parallel = 0$. The study of the polarization-dependent oscillator strengths of the interband transitions provide further information about the nature of the hole and electron states and state mixing.

### III. RESULTS

Figure 1 shows the energies of the first three lowest hole states in $(\text{GaAs})_n/(\text{AlAs})_n$ superlattices versus the superlattice period $n$ at $\mathbf{k}_\parallel = 0$. We see that the first three hole states have the order hh1, lh1, and hh2, respectively, and approach the GaAs VBM as the period $n$ increases. On the scale of the figure it is impossible to verify any anticrossing between lh1 and hh2. Thus, Fig. 2 shows a closeup of the region in the
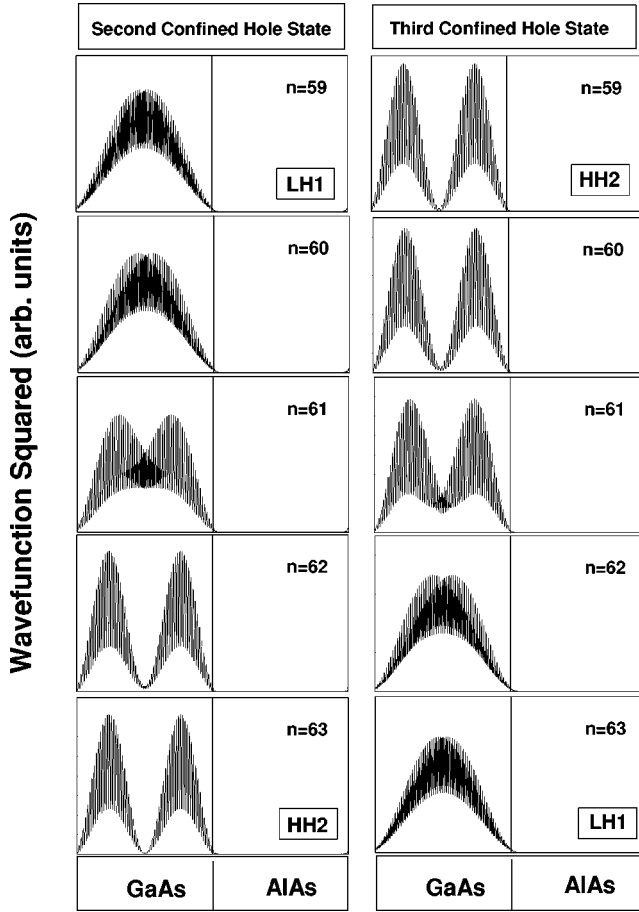
FIG. 3. Evolution of the wave functions of the second confined hole state left column) and the third confined hole states right column) of $(GaAs)_n/(AlAs)_n$ superlattices with the superlattice period $n$. Wave functions are averaged over the in-plane coordinates.

crossing period $n_c$ increases from a lower value $n_c=61$ at $E_v(x=1)=489$ meV to $n_c=66$ at $E_v(x=0.1)$ ▲ 40 meV.

Figure 6 shows the anticrossing gap $E_{AC}$ approximately twice the $V_{lh1,hh2}$ coupling parameter) versus the barrier height, $E_v(x)$. We obtain the largest value of $E_{AC}$ at

$E_v(x=0.2)=82$ meV. The corresponding coupling potential is $V_{lh1,hh2}$ 0.065 meV. Note that $V_{lh1,hh2}$ is smaller at higher $E_v$ higher Al content in the barrier) and is ↖ 0.03 meV at $E_v=490$ meV ($x=1$). Note also that these values for $V_{lh1,hh2}$ are larger than the value obtained in the case of $(GaAs)_n(AlAs)_n$ superlattices, 0.020 meV Fig. 2).

To understand the trend of the coupling $V_{lh1,hh2}$ versus barrier height, we refer to an expression derived by Cortez *et al.*[27] in the framework of the envelope-function description of the superlattice states:

$$V_{lh1,hh2} = \frac{E_v}{2\sqrt{3}} f_{lh1} \ z_{int}) f_{hh2} \ z_{int}) \frac{a}{2}.$$  (4)

In this model the coupling potential is taken to be proportional to the product of the envelope-function amplitudes $f_{lh1}$ and $f_{hh2}$ at the interfaces $z_{int}$ times the potential barrier value. To test this model we plot in Fig. 7 $(2V_{lh1,hh2})/(|f_{lh1}(z_{int})| \cdot |f_{hh2}(z_{int})|)$ versus $E_v(x)$. We use envelope functions $f$ which are directly extracted from our calculated microscopic wave functions, normalized over the unit-cell volume, through a macroscopic average procedure. In this procedure the wave functions are first averaged in the $xy$ planes orthogonal to the growth direction $z$ to obtain ‾$(z)$. Then, to eliminate the oscillations along the $z$ direction which are periodic with a period equal to a monolayer distance), ‾$(z)$ are averaged within every monolayer. The resulting envelopes $f$ are then normalized over the superlattice unit cell. We evaluate the envelopes $f(z)$ corresponding to superlattices with periods $n < n_c$, i.e., far from the anticrossing period where the lh1 and hh2 envelopes could be deformed by the coupling and extrapolate at $n_c$. According to the model of Cortez *et al.* the slope of Fig. 7 should be constant, $a/2\sqrt{3}$. Figure 7 shows that our microscopic calculation does not produce the simple linear scaling implied by Eq. 4). The function plotted increases rapidly at low valence-band offsets whereas at large offset it saturates to a constant value.
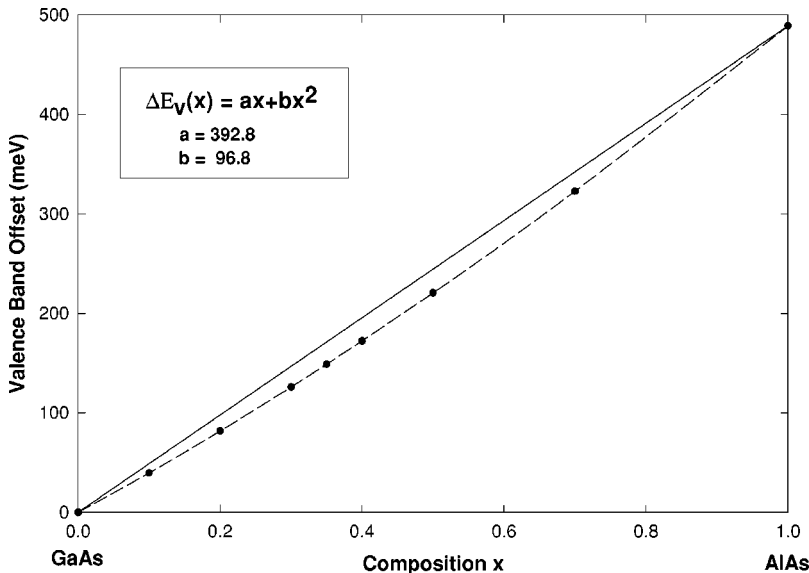


FIG. 4. Valence-band offset between the GaAs valence-band maximum and the $(Al_xGa_{1-x})As$ valence-band maximum as a function of the composition $x$ of the barrier.

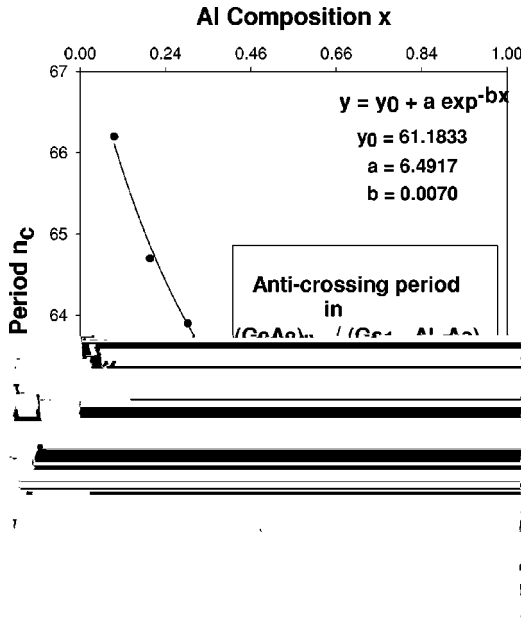FIG. 5. GaAs quantum well width $n_c$ at which the anticrossing between lh1 and hh2 occurs in $(GaAs)_n/(Al_xGa_{1-x}As)$ quantum wells as a function of the band offset $E_v(x)$ and the composition $x$ of the barrier.

We can analyze our results for $V_{lh1,hh2}$ versus $E_v$ as follows. For large barrier height the envelope functions are strongly localized *inside* the well, so their amplitude $f(z_{int})$ at the interfaces approaches zero, and $V_{lh1,hh2} \to 0$. For small barrier height $E_v \to 0$ there is no interface anymore, the cubic symmetry is restored, and $V_{lh1,hh2} \to 0$. Thus, there should be a value of $E_v$ at which the coupling matrix element $V_{lh1,hh2} = |\langle lh1 | V | hh2 \rangle|$ between lh1 and hh2 is largest. From Fig. 6 we see that the value of $E_v$ at which the coupling potential is largest is $E_v \approx 82$ meV (corresponding to $x \approx 0.2$). At higher $E_v$ values the coupling $V_{lh1,hh2}$ diminishes following the trend of the product of the amplitudes $f_{lh1}(z_{int}) \cdot f_{hh2}(z_{int})$ versus $E_v$ given in the inset of Fig. 7. At smaller $E_v$ the smaller potential change $V$ across the interface leads to a smaller coupling.
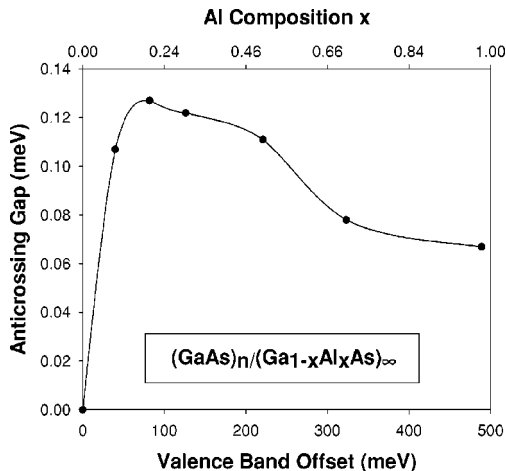


FIG. 6. Anticrossing gap ($\approx 2V_{lh1,hh2}$) vs the band offset between the GaAs well and the $(Al_xGa_{1-x})As$ barrier in $(GaAs)_n/(Al_xGa_{1-x}As)$ multiple quantum wells.
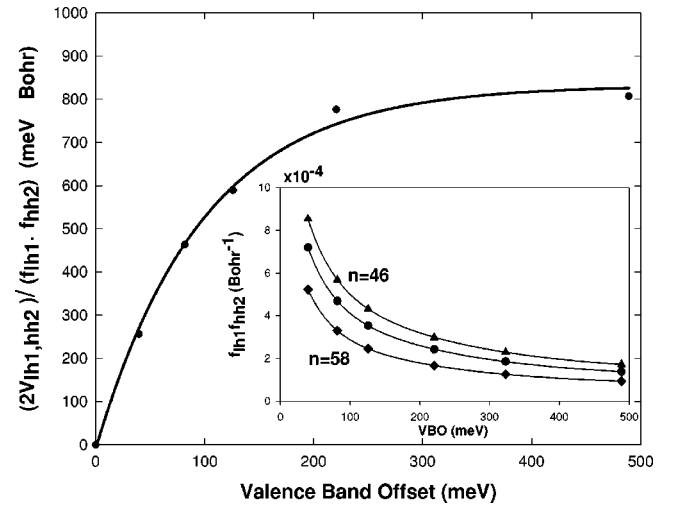


FIG. 7. Trend of the ratio between the coupling $V_{lh1,hh2}$ and the product of the lh1 and hh2 envelopes at the interface vs the band offset value in $(GaAs)_n/(Al_xGa_{1-x}As)$ multiple quantum wells. The best fit of the calculated points is obtained with an exponential function to be compared with the results of the simple model of Eq. 4). The inset shows the product of the envelope functions $f_{lh1}(z_{int}) \cdot f_{hh2}(z_{int})$ vs the band offset for different well widths $n$.

We see also that for $E_v < 200$ meV the Cortez *et al.*[17] formula is approximately followed. For $E_v > 200$ meV we find that $V_{lh1,hh2}$ follows the trend of the product $f_{lh1}(z_{int}) \cdot f_{hh2}(z_{int})$ times a costant, independent from the offset value.

## IV. COMPARISON WITH OTHER CALCULATIONS AND EXPERIMENT

We next compare our results for $V_{lh1,hh2}$ with the results of previous calculations. The first and only) atomistic calculation addressing the anticrossing of lh1 and hh2 at $\mathbf{k}_\parallel = 0$ in GaAs/AlAs is the work of Schulman and Chang[19,35] using an empirical tight-binding approach. To compare our calculated values with those reported by Schulman and Chang[35] we need to take into account the different parameters they used to describe the bulk compounds: $E_v(x=1) = 236$ meV our value is 489 meV) and for the effective masses of the light-hole and heavy-hole states $m_{hh}^{GaAs} = 0.45$, $m_{lh}^{GaAs} = 0.07$, $m_{hh}^{AlAs} = 0.75$, and $m_{lh}^{AlAs} = 0.15$, to be compared with our values given in Table II. Their offset value for the GaAs/AlAs heterojunction corresponds to that between GaAs and a $Al_xGa_{1-x}As$ barrier with $x \approx 0.5$ in our calculation see Fig. 4). For an infinite barrier with this composition we find anticrossing between lh1 and hh2 at a well width $n_c \approx 63$ monolayers and a gap value 0.11 meV, while Schulman and Chang found anticrossing at much smaller $n_c = 35$ monolayers. No values for the anticrossing gap were reported in their paper.

For a barrier with $m = 20$ monolayers of $Al_{0.3}Ga_{0.7}As$ which has an offset equal to a barrier of composition $x \approx 0.15$ in our calculation) they found anticrossing at a well width $n_c = 70$ monolayers. An anticrossing gap of fractions of meV can be estimated looking at Fig. 6 of Ref. 35. Thus, the order of magnitude of $V_{lh1,hh2}$ extracted from the tight-binding calculation of Schulman and Chang is in substantial

agreement with the values we have obtained with our pseudopotential approach. The different $n_c$ are related to the different bulk parameters.

Ivchenko *et al.*[6] considered a AlAs/GaAs/AlAs quantum well with a variable number $n$ of GaAs monolayers. They introduced the lh1 and hh2 anticrossing in an *ad hoc* fashion in the envelope-function formalism through the ''generalized boundary conditions,'' which are equivalent to adding to the Hamiltonian a -function term, localized at the interfaces. The coupling potential was expressed in terms of an adimensional parameter $t_{lh}$ multiplied by the product of the lh1 and hh2 envelope-function amplitudes at the interface. They used $m_{hh}=0.45$, $m_{lh}=0.09$, $E_v=0.53$ eV similar to our values $m_{hh}=0.40$, $m_{lh}=0.11$,▲ $E_v=0.49$ eV). Selecting $t_{lh}=0.5$ they obtained a gap of ▲–2 meV at the crossing point $n_c=50$. This gap is at least *one order of magnitude larger* than the values directly estimated in our atomistic calculations. Also, the trend of the $E_{lh1}$ and $E_{hh2}$ energies versus $n$, given in Fig. 3 a) of Ref. 6, is such that the minimum difference between them the anticrossing gap $E_{AC}$), is not achieved at $n=n_c$ the value of $n$ at which lh1 and hh2 exchange their character, see also Fig. 3 c) of Ref. 6] as it is in the atomistic calculations. Obviously, the interaction potential parameter $t_{lh}=0.5$ is too strong. Our atomistic calculations show that $V_{lh1,hh2}$ is smaller, of the order of tens or hundreds of meV, and its effect on the hole energies is seen essentially only at $n$ ➘ $n_c$. At smaller or larger $n$, $E_{lh1}=E_{lh1}^0$ and $E_{hh2}=E_{hh2}^0$, where $E_{lh1}^0$ and $E_{hh2}^0$ indicate the uncoupled lh1 and hh2 energies. The differences between the model Hamiltonian approach[6] and our atomistic approach highlight the fact that the former approach depends on parameters it cannot calculate.

On the experimental side, the effect of the lh1 and hh2 coupling in $D_{2d}$ systems is seen in the appearance of dipole-forbidden $e1$-hh2 and $e2$-lh1 exciton features.[17,18] From the excitation spectra of $(GaAs)_{36}/(Al_{0.27}Ga_{0.73}As)_{74}$ multiple quantum wells, the energy difference between the dipole-allowed $e_{1l}$ = (lh1-$e1$) and the dipole-forbidden $e_{12h}$ = (hh2-$e1$) excitons and between the dipole-forbidden $e_{21l}$ = (lh1-$e2$) and the dipole-allowed $e_{2h}$=(hh2-$e2$) excitons can be estimated in both cases to be about 10 meV. In our single-particle calculation when the splitting between $E_{lh1}$ and $E_{hh2}$ is 10 meV, the light-hole and heavy-hole states are only weakly coupled. However, a calculation of a full excitonic spectrum, which is beyond our single-particle approach, would be necessary to assess the intensities of these transitions and afford a direct comparison with this experiment.

## V. DIPOLE TRANSITION STRENGTHS

Figure 8 shows the dipole matrix elements for transitions from the second valence subband denoted as $V2$) and the third valence subband denoted as $V3$) to the two lowest conduction subbands, $e1$ and $e2$, for a $(GaAs)_n/(Al_{0.2}Ga_{0.8}As)_{m=74}$ quantum well, as a function of the number $n$ of GaAs layers in the well. We see that the dipole transition probabilities show a mirrorlike behavior across the value $n_c=64.7$ which corresponds to the calculated period $n_c$ of the anticrossing between lh1 and hh2. For $n<n_c$ the calculated transition probabilities indicate that the

subband $V2=$ lh1 and $V3=$hh2, while for $n>n_c$ the roles of $V2$ and $V3$ are exchanged. This calculation provides another way to study the mixing transition between $lh1$ and $hh2$ and determine the anticrossing point $n_c$. We see from this result that the transition takes place over just three monolayers. The calculations of Chang and Schulman[19] showed a much more gradual transition with the well width $n$.

From Fig. 8 we also see that there is a dependence of the transition probability on the polarization direction along $z$ or in the $x$-$y$ plane. The transitions to the $e2$ electron state are completely in-plane polarized while those to the $e1$ state are *mainly* polarized along $z$. No in-plane polarization anisotropy between the 110] and −110] directions is observed for any transitions. This can be understood by observing that the overall symmetry of these systems is the $D_{2d}$ point group which leads to anV2are

sary values for the coupling strength. We have calculated the strength of $V_{lh1,hh2}^{\mathbf{k}_\parallel=\mathbf{0}}$ through the evaluation of the anticrossing gap which opens between the lh1 and hh2 energies when they get closer to each other. This evaluation has been performed for $(GaAs)_n/(AlAs)_n$ superlattices and for $(GaAs)_n/(Al_xGa_{1-x}As)_{m=}$ quantum wells, where the Al content of the barrier $x$ has been varied from 0.1 to 1.0. At a critical period $n=n_c$, anticrossing between the lh1 and hh2 states is calculated. Our calculations show that the strength of $V_{lh1,hh2}$ is very small, of the order of magnitude 0.05 meV, in all the systems we have studied. The smallness of this interaction causes the lh1 and hh2 states to mix and form an anticrossing gap only for periods that are within a few monolayers of the critical size $n_c$ at which anticrossing occurs. This happens at a period $n_c^{\searrow}$ 61 in $(GaAs)_n/(AlAs)_n$ superlattices with a gap about 0.040 meV wide. Also in $(GaAs)_n/(Al_xGa_{1-x}As)_{m=}$ multiple quantum wells the anticrossing well width $n_c$ varies between 61 and 67 as a function of the Al barrier composition $x$. The anticrossing gap $E_{AC}$ and $V_{lh1,hh2}$) depends on the composition $x$ of the bar-